

## Supporting Information

### Retention and multiphase transformation of selenium oxyanions during the formation of magnetite via iron(II) hydroxide and green rust

Nicolas Börsig <sup>a,\*</sup>, Andreas C. Scheinost <sup>b,c</sup>, Samuel Shaw <sup>d</sup>, Dieter Schild <sup>e</sup>, Thomas Neumann <sup>a,f</sup>

<sup>a</sup> Karlsruhe Institute of Technology (KIT), Institute of Applied Geosciences, Adenauerring 20b, 76131 Karlsruhe, Germany

<sup>b</sup> Helmholtz-Zentrum Dresden-Rossendorf (HZDR), Institute of Resource Ecology, Bautzner Landstraße 400, 01328 Dresden, Germany

<sup>c</sup> The Rossendorf Beamline (ROBL) at ESRF, 38043 Grenoble, France

<sup>d</sup> The University of Manchester, School of Earth, Atmospheric and Environmental Sciences, Manchester, M13 9PL, United Kingdom

<sup>e</sup> Karlsruhe Institute of Technology (KIT), Institute for Nuclear Waste Disposal, Hermann-von-Helmholtz-Platz 1, 76344 Eggenstein-Leopoldshafen, Germany

<sup>f</sup> Technical University of Berlin, Institute of Applied Geoscience, Ernst-Reuter-Platz 1, 10587 Berlin, Germany

\*Corresponding author: Tel.: +49 721 608-44878; nicolas.boersig@kit.edu (N. Börsig)

## 1 Information about analytical techniques

### 1.1 ICP-OES and ICP-MS

After centrifugation and filtration (0.2 µm filter), all supernatants were acidified with concentrated high-purity HNO<sub>3</sub> (50 µL). The Se and Fe concentrations in the aqueous phase were determined by ICP-OES (Inductively Coupled Plasma Optical Emission Spectrometry) or ICP-MS (Inductively Coupled Plasma Mass Spectrometry) depending on the concentrations: For amounts higher than 1 mg/L, measurements were performed on ICP-OES using a Varian 715ES. Analysis of samples with lower Fe and Se concentrations were carried out on an X-Series 2 ICP-MS (Thermo Fisher Scientific Inc.).

In case of ICP-MS analysis collision cell mode was used to eliminate polyatomic clusters, and Se and Fe isotopes (m/z: 76, 77, 78 for Se; 56 for Fe) without spectroscopic interferences were selected for detection. <sup>45</sup>Sc, <sup>103</sup>Rh, and <sup>115</sup>In were used as internal standards to minimize non-spectroscopic interferences. This includes the correction of signal changes caused by high ionic strength in some of the sample matrices.

The lower detection limits were approx. 0.3 µg/L for both Se and Fe. Throughout the analyses of both ICP methods, a certified reference solution was used as standard.

## 1.2 XRD

X-Ray Diffraction (XRD) was used for analysis of the purity and composition of the synthesized solid materials and performed on a Bruker D8 Advance X-ray diffractometer with Cu K $\alpha$  radiation ( $\lambda = 1.5406 \text{ \AA}$ ) and a LynxEye detector. Magnetite samples (reaction time: 48 h) were prepared from powders. By contrast, the redox-sensitive, undried samples of the initial precipitation products (magnetite precursor; reaction time: 30 min or 3 h) were analyzed in their original form as solid-rich suspension (sludge). This was done to avoid further oxidation of this sample type due to air contact during the alternative drying step or the XRD analysis itself. XRD patterns of the analyzed samples were compared with mineral references of the ICDD PDF-2 database.

## 1.3 BET

BET measurements were conducted on pure magnetite as well as on its precursor phase using a Quantachrome Autosorb 1-MP and 11-point BET-argon isotherms recorded at the temperature of liquid argon (87.3K) to calculate the specific surface areas (SSA). Prior to the measurement, the sample were outgassed in vacuum at 95°C overnight to remove water and other volatile surface contaminations. Note that the sample drying might has changed the characteristics of the solid phase in case of the redox-sensitive magnetite precursor phase.

## 1.4 pEDXRF

The Se content of the solid phases was determined by polarized Energy Dispersive X-ray Fluorescence Spectroscopy (pEDXRF) using an Epsilon 5 (PANalytical) equipped with a W X-ray tube and a Ge detector. A Mo target was selected as polarizing secondary target and the measurement period was 500 s, resulting in a lower detection limit for Se of 10 ppm and an analytical precision of  $\pm 5 \text{ \%}$ . Prepared standards consisting of mixtures of synthesized pure hematite and known amounts of a Se reference material (pure Se(0) powder or certified Se reference solution) were utilized for calibration.

## 1.5 SEM & EDX

SEM images were obtained using a LEO 1530 (Zeiss Inc.) scanning electron microscope (operated at 10 kV) with a NORAN System SIX (Thermo Electron Corp.) EDX-System. The dried powder samples (reaction time: 48 h) were coated with Pt after they were mounted on sample holders via double-sided carbon tape.

Increased levels of C and Pt in EDX spectra are due to the characteristics of the sample holders and the Pt coating of the samples.

## 1.6 S/TEM & EDX

S/TEM images were recorded using a FEI Talos F200X analytical scanning/transmission electron microscope (operated at 200 kV) equipped with an integrated Super-X EDS system with 4 windowless silicon drift detectors (SDD). S/TEM samples were prepared in an oxygen-free glove box by directly pipetting fresh samples of the magnetite precursor phase onto the TEM grid followed by a few drops of isopropanol to wash off excess salt. Holey-carbon Cu mesh grids (200 mesh) were used as sample holders.

Increased levels of Cu, Au and C in EDX spectra are due to the use of holey-carbon Cu mesh grids.

## 1.7 XPS

XPS measurements were performed using a PHI 5000 VersaProbe II (ULVAC-PHI Inc.). The system was equipped with a scanning microprobe X-ray source (monochromatic Al K $\alpha$ , 1486.7 eV) in combination with an electron flood gun and a floating ion gun generating low-energy electrons (1.1 eV) and low energy argon ions (8 eV) for charge compensation at isolating samples (dual beam technique), respectively. Calibration of the binding energy scale of the spectrometer was performed using the well-established binding energies of elemental lines of pure metals (monochromatic Al K $\alpha$ : Cu 2p<sub>3/2</sub> at 932.62 eV, Au 4f<sub>7/2</sub> at 83.96 eV<sup>1</sup>. O1s ( $\alpha$ -Fe<sub>3</sub>O<sub>4</sub>) at 530.0 eV or O1s (OH) at 531.2 eV were used as charge reference for the analyzed samples<sup>2</sup>. Error of binding energies of elemental lines is estimated to  $\pm$  0.2 eV. Samples were moved without air contact from the anoxic glovebox into the XP spectrometer by means of a transfer vessel (ULVAC-PHI Inc.). Data analysis was performed using ULVAC-PHI MultiPak program, version 9.6.

## 1.8 XAS

For XAS analysis at ROBL, a 13 element high-purity germanium detector (Canberra) with digital signal processing (XIA) for fluorescence detection was used. The monochromator energy was calibrated with a gold foil (K-edge at 11919 eV) because of its greater inertness and hence reliability in comparison to elemental Se. During the sample preparation, small amounts of Se-bearing magnetite powders or, in case of the magnetite precursor phase, small amounts of a solid-rich suspension were placed in sample holders and sealed with Kapton® tape. Spectra were collected at 15 K using a closed cycle He cryostat with a large fluorescence exit window and a low vibration level (CryoVac) in order to avoid photon-induced redox reactions.

## 2 Results

### 2.1 Characterization of synthesized magnetite and its precursor phases

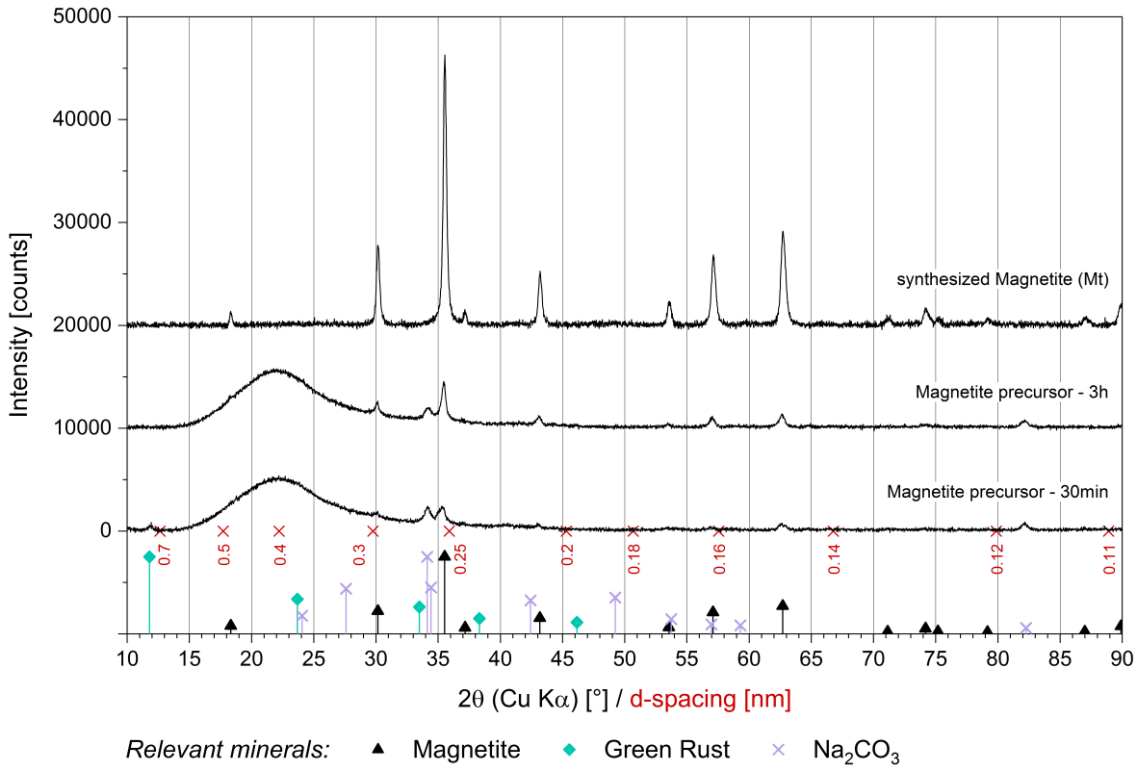


**Fig. A.1** XRD results of the pure synthesis products – magnetite and its precursor phases.

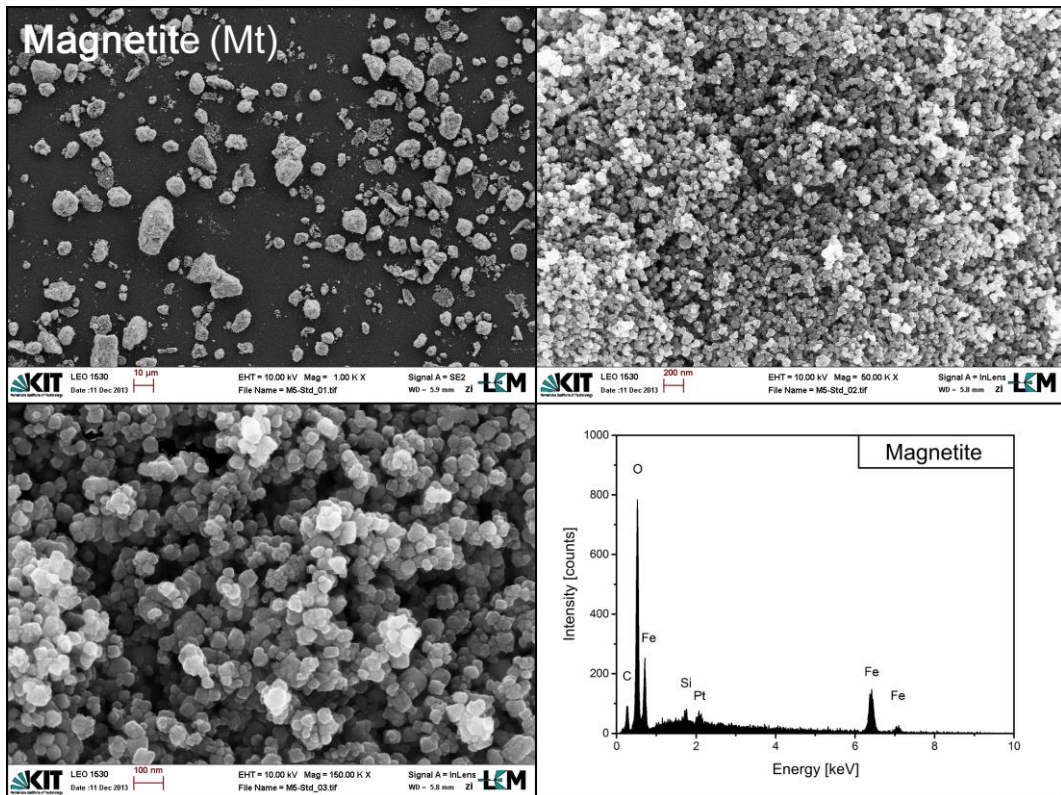


**Fig. A.2** SEM/EDX results of a pure magnetite phase. EDX spectra shows the result of a bulk analysis.

## 2.2 Characterization of the coprecipitation products within the Fe-Se-H<sub>2</sub>O system during or following the formation of magnetite

**Table A.1 Crystallographic data of used selenium references for XRD and XAS analysis/evaluation**

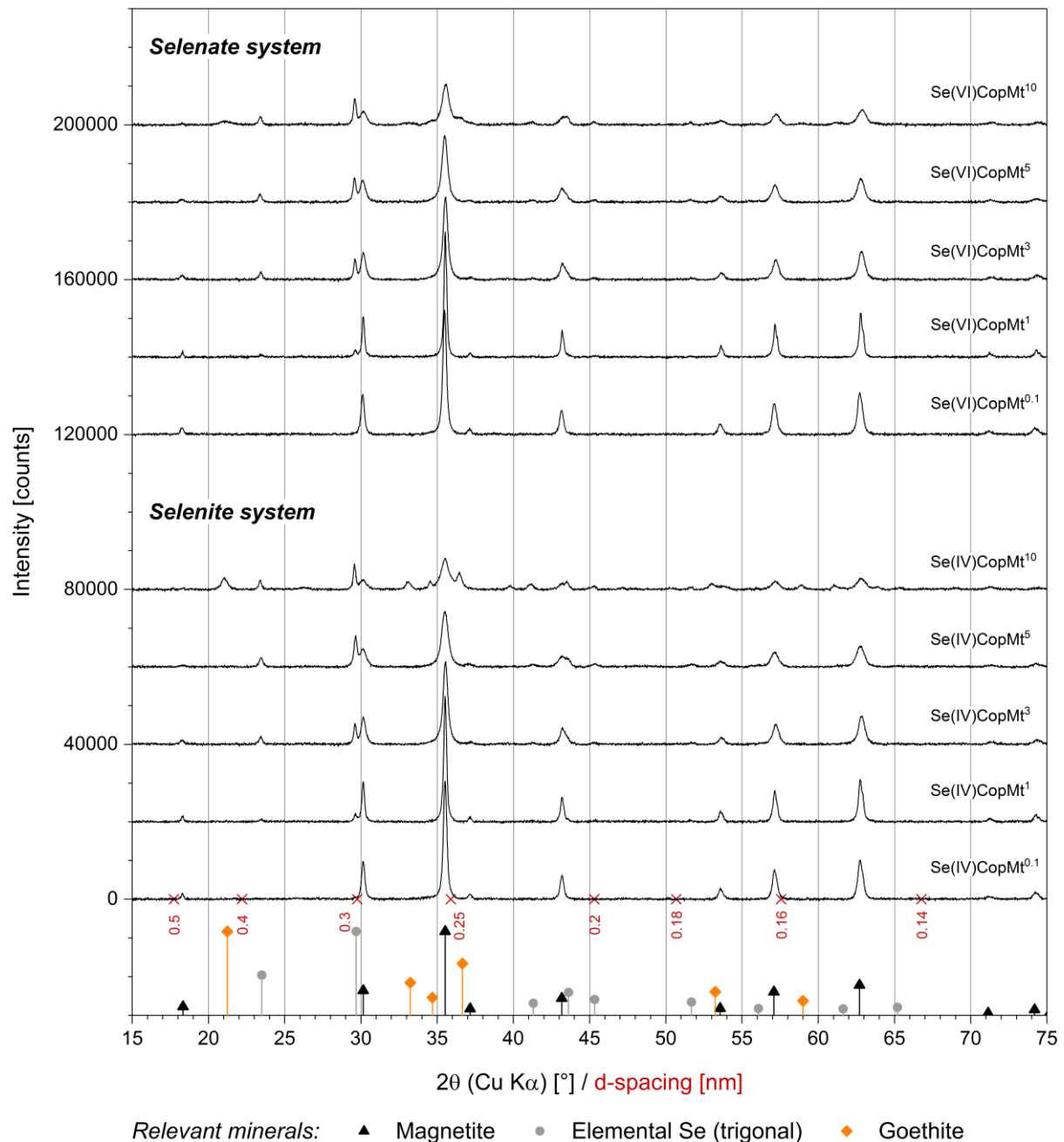
<b>Elemental selenium reference for XRD analysis</b>	
PDF number	86-2246
Name	Gray trigonal selenium
Formula	Se
Crystal system	Trigonal
Space Group	P 3 <sub>1</sub> 2 1 (152)
Lattice parameters	
a	4.368 Å
c	4.958 Å
Volume	81.92 Å <sup>3</sup>
Z	3
Density	4.80 g/cm <sup>3</sup>
Structure reference	Keller R., Holzapfel W.B., Schulz H. (1977) Phys. Rev. B16, 4404-4412
Reference	Calculated from ICSD using POWD-12++ (1997)

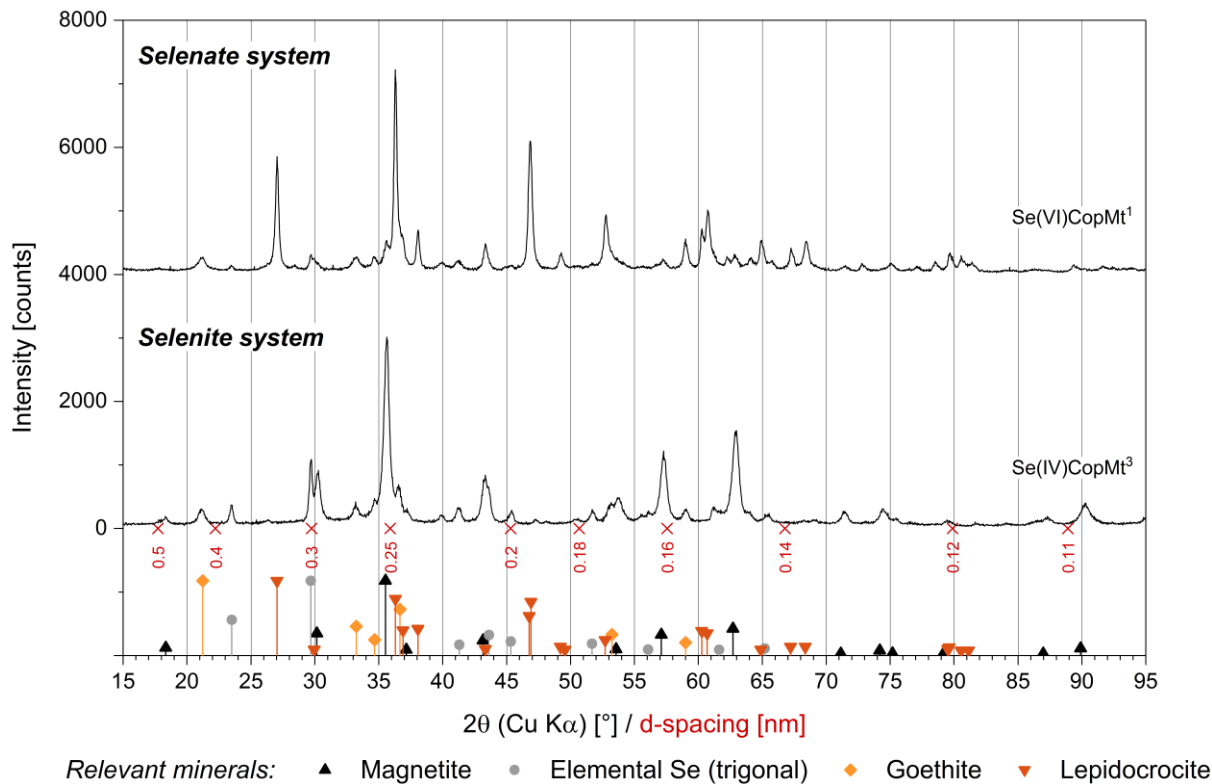
<b>Elemental selenium reference for XAS analysis</b>	
ICSD code (CIF)	22251
Name	Gray trigonal selenium
Formula	Se
Crystal system	Trigonal
Space Group	P 3 <sub>1</sub> 2 1 (152)
Lattice parameters	
a	4.366 Å
c	4.954 Å
Volume	81.78 Å <sup>3</sup>
Z	3
Density	4.81 g/cm <sup>3</sup>
Reference	Cherin P. and Unger P. (1967) Inorg. Chem. 6, 1589-1591

<b>Iron(II) selenide reference for XAS analysis</b>	
ICSD code (CIF)	26889
Name	Iron selenide
Formula	FeSe
Crystal system	tetragonal
Space Group	P 4/n m m (129)
Lattice parameters	
a	3.765 Å
c	5.518 Å
Volume	78.22 Å <sup>3</sup>
Z	2
Density	5.72 g/cm <sup>3</sup>
Reference	Haegg G. and Kindstroem A.L. (1933) Z. Phys. Chem. B, 22, 453–464



**Fig. A.3** XRD results of magnetite (Mt) samples of coprecipitation (Cop) experiments with selenite [Se(VI)] and selenate [Se(VI)]. Initial Se concentrations: "X"  $c(\text{Se})_0 = "X" \cdot 10^{-3} \text{ mol/L}$ .



**Fig. A.4** XRD results of comparative magnetite coprecipitation experiments with selenite [Se(IV)] or selenate [Se(VI)], where the coprecipitation process led to the formation of magnetite and iron(III) oxyhydroxide (goethite and/or lepidocrocite) mixed phases. Initial Se concentrations: “X”  $c(\text{Se})_0 = "X" \cdot 10^{-3}$  mol/L.

**Table A.2** XPS results of magnetite samples from coprecipitation experiments with selenite or selenate as well as pure magnetite (all unwashed): Atomic concentrations (at%) of main elements;  $x_{\text{Fe(II)}}$ : Fe(II)/Fe<sub>total</sub> ratio; Binding energies in eV.  
 “X”  $c(\text{Se})_0 = "X" \cdot 10^{-3}$  mol/L; \* magnetite precursor; # Determined by comparison with the published Fe 2p spectra of stoichiometric GR(CO<sub>3</sub><sup>2-</sup>), Mullet *et al.*<sup>6</sup>, cf. Fig. A.6.

Sample	C	N	O	Na	Cl	K	Fe	Se	$x_{\text{Fe(II)}}$
Se(IV)CopMt¹-30min *	5.6	---	60.9	1.0	1.1	2.2	28.5	0.6	~0.67 #
Se(VI)CopMt¹-30min *	11.3	---	51.5	5.6	5.5	5.6	20.2	0.3	~0.67 #
Magnetite (pure)	9.5	0.6	53.1	1.3	0.7	3.0	31.8	---	0.14
Se(IV)CopMt¹	5.0	---	53.8	0.9	0.8	1.5	37.3	0.7	0.13
Se(VI)CopMt¹	12.9	---	51.4	0.8	1.6	1.8	30.8	0.7	0.09

At.-%: relative error  $\pm 10\text{-}20\%$ .  $x_{\text{Fe(II)}}$ : relative error  $\pm 5\%$ .

Sample	Se 3s	Se L <sub>3</sub> M <sub>45</sub> M <sub>45</sub>	Se 3p <sub>3/2</sub>	Se L <sub>2</sub> M <sub>45</sub> M <sub>45</sub>	O 1s (charge ref.)	Se valency
Se(IV)CopMt¹-30min *	228.2	178.6	159.9	137.6	531.2	OH
Se(VI)CopMt¹-30min *	228.3	178.8	159.8	137.6	531.2	OH
Se(IV)CopMt¹	229.8	179.2	161.2	137.9	530.0	Fe <sub>3</sub> O <sub>4</sub>
Se(VI)CopMt¹	230.0	179.0	161.1	137.9	530.0	Fe <sub>3</sub> O <sub>4</sub>

Binding energy: error  $\pm 0.2$  eV

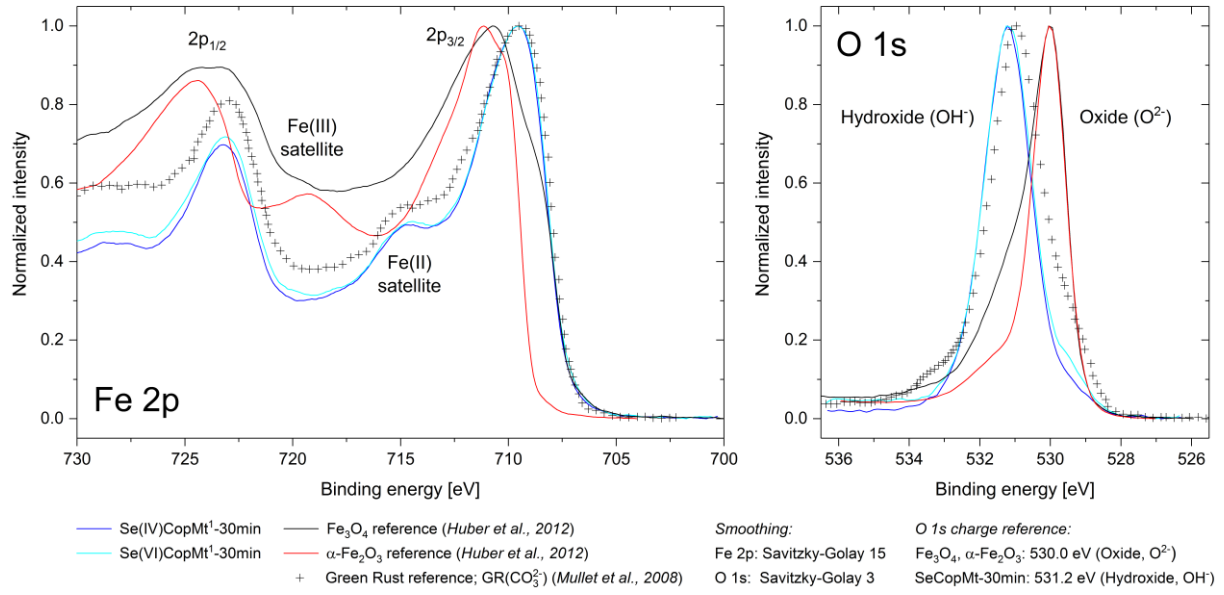


**Fig. A.5** Comparison between XPS spectra of Selenite-magnetite and Selenate-magnetite coprecipitation products after a reaction time of 30 minutes and different iron oxide references <sup>6,7</sup>.

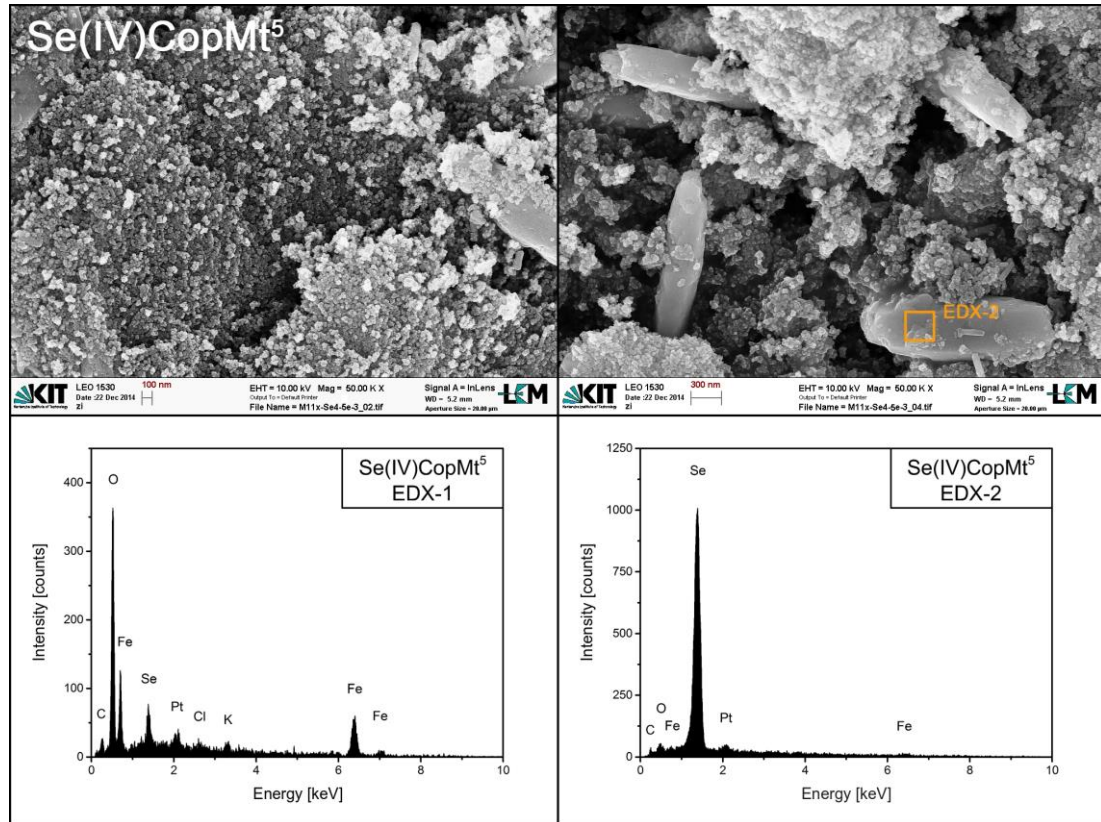


**Fig. A.6** SEM/EDX results of Selenite-magnetite coprecipitation products consisting of elemental Se crystals in a matrix of magnetite;  $c(\text{Se})_0 = 5 \cdot 10^{-3}$  mol/L. Spectra EDX-1 shows the result of a bulk analysis; Spot of spectra EDX-2 is shown in the SEM image.

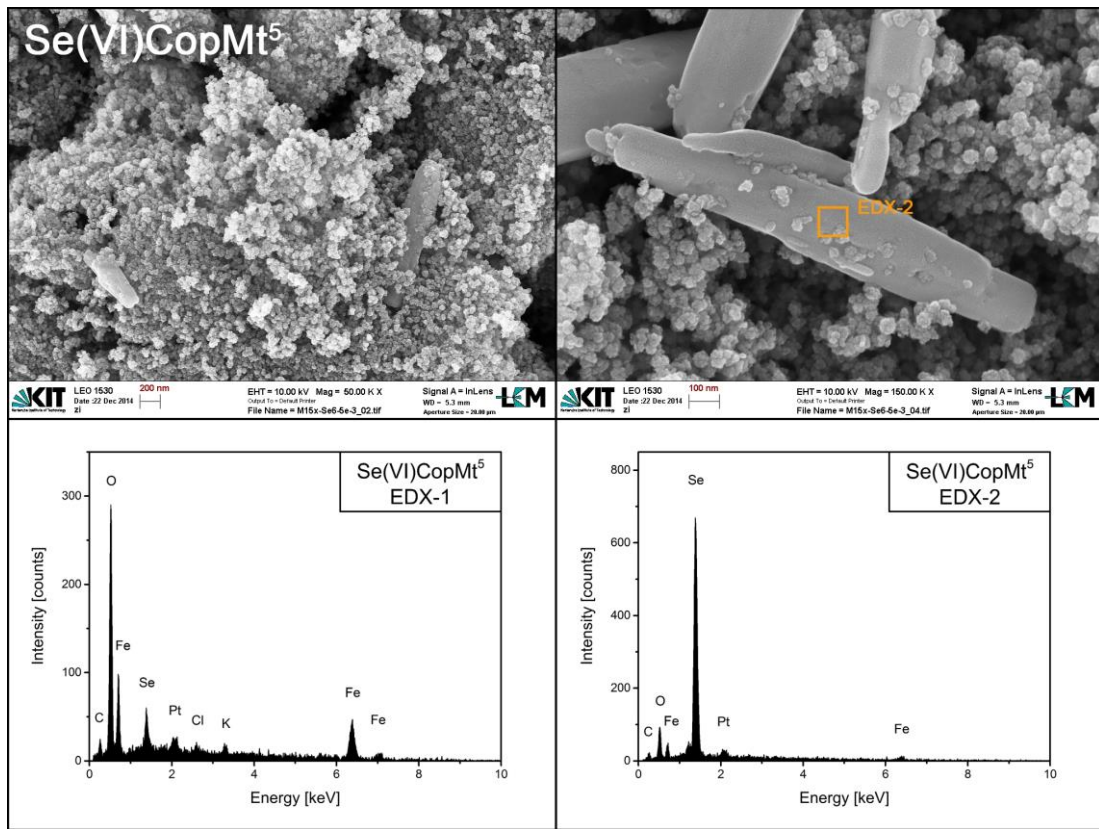


**Fig. A.7** SEM/EDX results of Selenate-magnetite coprecipitation products consisting of elemental Se crystals in a matrix of magnetite;  $c(\text{Se})_0 = 5 \cdot 10^{-3}$  mol/L. Spectra EDX-1 shows the result of a bulk analysis; Spot of spectra EDX-2 is shown in the SEM image.

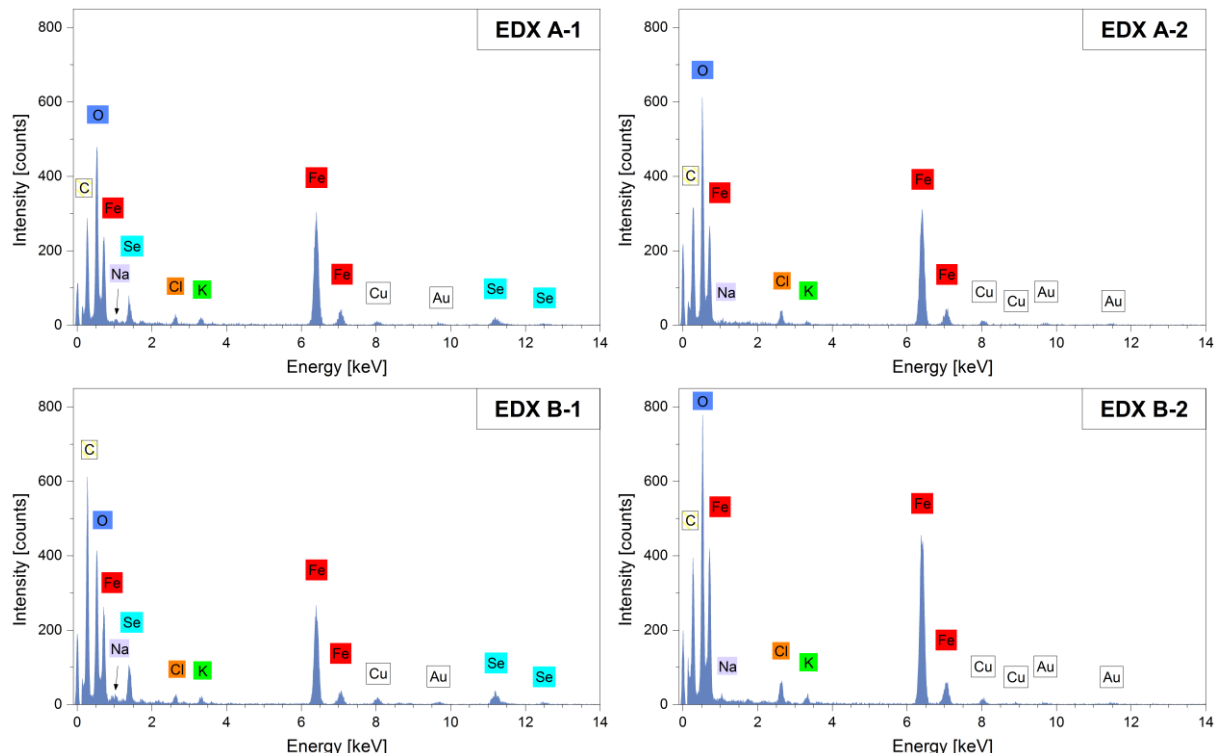


**Fig. A.8** EDX spectra of Se-rich (FeSe) and Se-free (Green Rust) compounds of a Selenite-magnetite coprecipitation product after a reaction time of 30 min. Spots of spectra are shown in Fig. 5.

## References

- 1 M. P. Seah, I. S. Gilmore and G. Beamson, *Surf. Interface Anal.*, 1998, **26**, 642–649.
- 2 J. F. Moulder, W. F. Stickle, P. E. Sobol and K. D. Bomben, *Handbook of X-ray Photoelectron Spectroscopy*, ULVAC-PHI, Inc. (Japan); Physical Electronics USA, Inc., 1995.
- 3 R. Keller, W. B. Holzapfel and H. Schulz, *Phys. Rev. B*, 1977, **16**, 4404–4412.
- 4 P. Cherin and P. Unger, *Inorg. Chem.*, 1967, **6**, 1589–1591.
- 5 G. Haegg and A. L. Kindstroem, *Z. Phys. Chem. B*, 1933, **22**, 453–464.
- 6 M. Mullet, Y. Guillemin and C. Ruby, *J. Solid State Chem.*, 2008, **181**, 81–89.
- 7 F. Huber, D. Schild, T. Vitova, J. Rothe, R. Kirsch and T. Schäfer, *Geochim. Cosmochim. Acta*, 2012, **96**, 154–173.